International Science and Technology Journal
المجلة الدولية للعلوم والتقنية
Volume 37 العدد
Part 2 المجلد
ISTJ
http://www.doi.org/10.62341/smza1125

Received	**2025/10/29**	**تم استلام الورقة العلمية في**
Accepted	**2025/11/20**	**تم قبول الورقة العلمية في**
Published	**2025/11/21**	**تم نشر الورقة العلمية في**

The Stability of Silver Nanoparticles and Their Antibacterial Activity against *Escherichia Coli*

Sana Abdulkhader[1], Mohammed Ahwidi, Zenab Abdoorhman[2], Mohamed Erhayem[1] and Aisha AL-Abbasi[*1]

[1]Department of Chemistry, Faculty of Science, Sebha University, Libya
[2]Department of Zoology, Faculty of Science, Sebha University, Libya

[*]Corresponding Author: ais.alabbasi@sebhau.edu.ly

Abstract

Silver nanoparticles (AgNPs) have fascinated significant attention because of their wide range of biological and industrial applications. In this study, reports the synthesis, and assessment of the stability and antibacterial capability of silver nanoparticles (AgNPs) synthesized via sodium borohydride ($NaBH_4$) and stabilized by sodium dodecyl sulfate (SDS). AgNPs were prepared at varying silver nitrate ($AgNO_3$) concentrations (0.1, 0.2, 0.5, and 1.0 mM) and confirmed by UV-Vis spectroscopy, which revealed surface plasmon resonance (SPR) peaks ranging from 393 to 411 nm, depending on precursor concentration. The SPR intensity increased with both $AgNO_3$ concentration and temperature, with maximum absorbance values reaching 3.57 $L \cdot mol^{-1} \cdot cm^{-1}$ at 1.0 mM $AgNO_3$ and 100°C. Time-based stability tests showed that AgNPs retained optical stability for over 120 days, with minimal peak broadening and a slight red shift in λ_{max}. pH-dependent studies revealed optimal stability at pH 7–8, while aggregation was observed at 1–2 pH and pH 13. Antibacterial assays against *Escherichia coli* demonstrated strong inhibition, with zones of inhibition increasing from 1 mm at 0.1 mM to 2 mm at 1.0 mM. The results confirm that AgNPs synthesized under optimized conditions are both stable and highly effective as antibacterial agents, supporting their potential application in nanomedicine and environmental disinfection.

Keywords*:* Silver nanoparticles, UV-V Surface plasmon resonance, SDS stabilizer, Time and pH stability, Antibacterial, *Escherichia coli.*

International Science and Technology Journal
المجلة الدولية للعلوم والتقنية
Volume 37 العدد
Part 2 المجلد
http://www.doi.org/10.62341/smza1125

استقرار جزيئات الفضة النانوية ونشاطها المضاد للبكتيريا ضد الإشريكية القولونية

سناء عبد القادر[1]، محمد هويدي[1]، زينب عبد الرحمن[2]، محمد إرحيم[1] وعائشة العباسي[1*]

[1]قسم الكيمياء، كلية العلوم، جامعة سبها، ليبيا
[2]قسم علم الحيوان، كلية العلوم، جامعة سبها، ليبيا

ملخص

جذبت جزيئات الفضة النانوية (AgNPs) اهتمامًا كبيرًا بسبب تنوع تطبيقاتها البيولوجية والصناعية. في هذه الدراسة، يتم الإبلاغ عن توليف وتقييم استقرار وقدرة جزيئات الفضة النانوية (AgNPs) المركبة عبر بوروهيدريد الصوديوم ($NaBH_4$) والمثبتة بواسطة ثنائي سلفات الصوديوم .(SDS) تم تحضير جزيئات AgNPs بتركيزات متفاوتة من نترات الفضة 0.1) ($AgNO_3$) و 0.2 و 0.5 و 1.0 مليمول) وتم تأكيدها بواسطة التحليل الطيفي للأشعة فوق البنفسجية والمرئية(UV–Vis) ، الذي كشف عن قمم رنين البلازمون السطحي (SPR) تتراوح من 393 إلى 411 نانومتر، اعتمادًا على تركيز السلائف. زادت شدة SPR مع كل من تركيز $AgNO_3$ ودرجة الحرارة، حيث وصلت قيم الامتصاص القصوى إلى 3.57 $L \cdot mol^{-1} \cdot cm^{-1}$ عند 1.0 مليمول $AgNO_3$ و 100 درجة مئوية. أظهرت اختبارات الاستقرار الزمني أن جزيئات AgNPs احتفظت باستقرارها البصري لأكثر من 120 يومًا، مع توسع طفيف في الذروة وتحول طفيف إلى اللون الأحمر في λmax. كشفت الدراسات المعتمدة على درجة الحموضة عن استقرار أمثل عند درجة حموضة 7–8، بينما لوحظ تكتل عند درجة حموضة 1–2 ودرجة حموضة 13. أظهرت الاختبارات المضادة للبكتيريا ضد Escherichia coli تثبيطًا قويًا، مع زيادة مناطق التثبيط من 1 مم عند 0.1 مليمولار إلى 2 مم عند 1.0 مليمولار. تؤكد النتائج أن جزيئات AgNPs المُصنعة في ظل ظروف مُحسّنة هي مستقرة وفعالة للغاية كعوامل مضادة للبكتيريا، مما يدعم تطبيقها المحتمل في الطب النانوي وتطهير البيئة.

الكلمات المفتاحية: جزيئات الفضة النانوية، رنين البلازمون السطحي UV–V، مثبت SDS، الاستقرار الزمني واستقرار درجة الحموضة، مضاد للجراثيم، الإشريكية القولونية.

http://www.doi.org/10.62341/smza1125

Introduction

Among its most promising innovations are metallic nanoparticles, particularly silver nanoparticles (Emma, 2025; Haleem, Javaid, Singh, Rab, & Suman, 2023), which have involved significant interest due to their exceptional properties. These consist of its chemical stability, electrical, optical and catalytic capability, and potent biological effects (Abbas et al., 2024; Dhaka, Chand Mali, Sharma, & Trivedi, 2023; Oleksandra et al., 2021). AgNPs are extensively employed in wound dressings, medicine delivery systems, packaging foodstuff, water purification, and healthcare goods. Ag nano can be produced using physical, chemical, or biological means, with reduction technology being the greatest adopted (Duman et al., 2024; Fernando, 2018; Mavani & Shah, 2013; Nyabadza et al., 2023; Oleksandra et al., 2021). This method utilizes ($NaBH_4$), ascorbic acid, and alcohols, supported by stabilizing agents like dodecyl sulfate sodium salt (SDS), dimethylformamide (DMF), or polyethylene glycol (PEG) to control particle size and prevent aggregation (Ahmed, Ahmad, Swami, & Ikram, 2016; Wei et al., 2015; Oleksandra et al., 2021). $NaBH_4$, in particular, is a strong reducing agent that facilitates the rapid formation of Ag^0, which subsequently aggregate into nanoparticles. Stabilizers such as SDS generate repulsive forces that maintain uniform dispersion and functional integrity of the nanoparticles (Ali, Omar, & Al-Abbasi, 2025; Mavani & Shah, 2013). Despite their versatility, AgNPs in free form are thermodynamically unstable due to their high surface energy and Brownian motion, which promote agglomeration. Stability is governed by the interplay between attractive Van der Waals forces and repulsive interactions (electrostatic or steric), with effective stabilization preventing aggregation and maintaining colloidal dispersion (Güzel & Erdal, 2018). Environmental conditions such as pH, temperature, and storage duration play a crucial role in the physicochemical behavior, stability, and functionality of AgNPs (Duman et al., 2024; Fernando, 2018; Güzel & Erdal, 2018; Mavani & Shah, 2013). The effectiveness of AgNPs— versus bacteria mainly versus Gram-negative bacteria like *Escherichia coli*—has received extensive attention due to their ability to disrupt microbial membranes, interfere with intracellular processes, and ultimately lead to cell deat (Dhaka et al., 2023; Emma, 2025; Haque, 2017;

http://www.doi.org/10.62341/smza1125

Oleksandra et al., 2021). Their mechanism of action includes interaction with sulfur- and phosphorus-containing biomolecules (e.g., proteins and DNA), binding to membrane proteins, and the discharge of silver cations that compromise essential cellular functions (González-Fernández et al., 2025; More et al., 2023). AgNPs are effective versus a wide kind of microorganisms, as antibiotic-resistant strains (Hosseini et al., 2025; Shrestha, Wang, & Dutta, 2020). Factors influencing their antimicrobial capability include surface chemistry, particle size and shape, ion release rate, and the type of microbial cell (Anees Ahmad et al., 2020; Carlson et al., 2008; Zhang, Liu, Shen, & Gurunathan, 2016).

AgNPs are extensively applied in wound dressings, drug delivery systems, and water purification technologies. Silver nanoparticles are extensively applied in medicine fields, nutrition safety, healthcare, and, goods (Bruna, Maldonado-Bravo, Jara, & Caro, 2021; Rodrigues et al., 2024; Sati, Ranade, Mali, Ahmad Yasin, & Pratap, 2025). Additionally, the antimicrobial action of AgNPs like *Escherichia coli*, has attracted considerable interest. This widespread use is attributed to their unique characteristics, including stability, high conductivity, optical responsiveness, catalytic behavior, and biological capability. Several recent studies have focused on optimizing the synthesis and evaluating the stability and antimicrobial properties of AgNPs using different methods. Chandirika et al. (2018) described a eco-friendly production system using *Abutilon indicum*, observing strong antimicrobial capability and a UV-visible absorption peak at ~420 nm (Jayaram & Gurusamy, 2018). Boroumand et al. (2018) synthesized AgNPs via chemical reduction with $NaBH_4$ and pomegranate peel extract, achieving broad pH stability and antimicrobial efficacy (Nasiriboroumand, Montazer, & Barani, 2018). Velgosova et al. (2017) used algae-based synthesis and noted stability lasting 4 to 30 days with peak absorbance at 415 nm (Velgosova, Čižmárová, Málek, & Kavuličova, 2017). Haque et al. (2017) used polyvinyl pyrrolidone (PVP) as a stabilizer and demonstrated that AgNPs maintained stability under varying oxidative and thermal conditions, with characteristic UV-visible peaks between 390–420 nm (Haque, 2017).

Aligned with our interest in nanoparticle research (Ali et al., 2025; Almutaleb & Alabbasi, 2023; Dnkm, Al-Abbassi, & Erhayem,

http://www.doi.org/10.62341/smza1125

2024; S. Khalifa, AL-abbassi, & Suliman, 2019; Salim, Izriq, Almaky, & Al-Abbassi, 2022; Suhud et al., 2015)**,** this study aims to synthesize silver nanoparticles via chemical reduction, assess their physicochemical stability under different environmental conditions, and estimate their antimicrobial versus *E. coli*. The findings pay to the increasing the knowledge of nanoparticle behavior, supporting future applications in antimicrobial technologies and nanomedicine.

Experimental Section

Materials and Instrumentation

In the current study, high-purity, analytical-grade chemicals were utilized to ensure the reliability and accuracy of the experimental outcomes. Silver nitrate ($AgNO_3$), the primary precursor for nanoparticle synthesis, was obtained from Scarl. Sodium borohydride ($NaBH_4$), serving as the reducing agent, was sourced from BDH. Additionally, sodium dodecyl sulfate (SDS), a surfactant and stabilizing agent, was procured by Aldrich.

The characterization and monitoring of the synthesized AgNPs were established using advanced analytical instrumentation. A UV-Visible (UV-Vis) spectrophotometer (Evolution 300, Thermo Electron Corporation) was utilized to record the optical properties of the surface plasmon resonance (SPR) characteristics. Furthermore, a digital pH meter (Thermo Orion 4-Star model) was utilized to estimate the pH of solutions with precision during various stages of synthesis and stability testing. The combination of these high-quality chemicals and precise analytical instruments contributed to the reproducibility and accuracy of the experimental procedures and results.

Silver Nano scales Synthesis

Nano silver was produced by utilizing borohydride sodium and dodecyl sulfate sodium salt as the stabilizing surfactant. To begin, aqueous solutions of $AgNO_3$ were prepared at 0.1 mM, 0.2 mM, 0.5 mM, and 1.0 mM concentrations. In parallel, SDS and $NaBH_4$ were each dissolved in deionized water to obtain 1, 2, 5, and 10 mM concentrations, respectively. The nanoparticle synthesis was carried out by the addition of drops of the $AgNO_3$ into the NaBH/SDS mixture, under continuous magnetic stirring. The reaction mixture

http://www.doi.org/10.62341/smza1125

was stirred for a period of 90 minutes to confirm complete reduction and stabilization.

The procedure was sustained at a molar ratio of $NaBH_4$ to $AgNO_3$ of 10:1, and a weight ratio of SDS to $AgNO_3$ of 2:1, which were establish to be optimum for fabricating stable and well-dispersed nano silver. Subsequent the production, the formation and optical properties were examined and established by recording the UV-Visible absorption spectra for each trial, converging the distinctive surface plasmon resonance (SPR) peaks revealing of nanoparticle establishment (Figure 1).

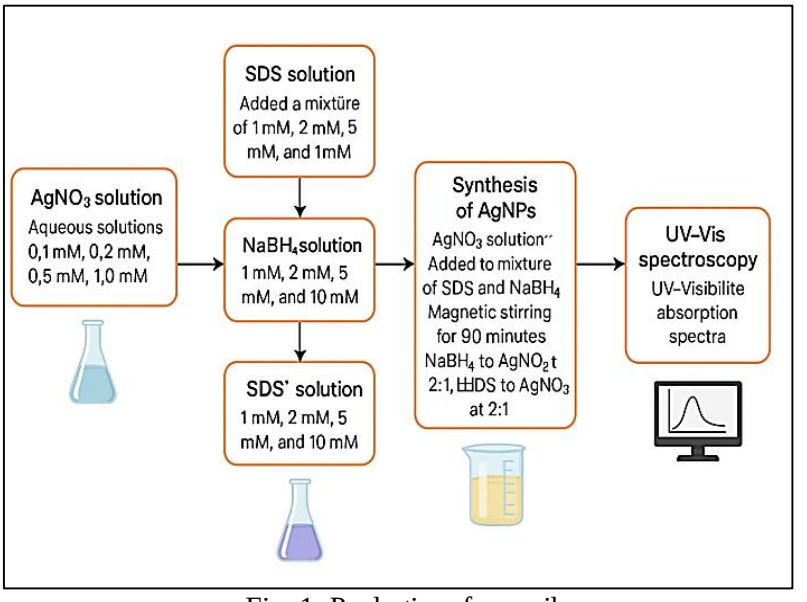

Fig. 1: Production of nano silver

Stability Assessment under Time, Temperature, and pH Variations

The stability of the produced AgNPs was methodically investigated under changeable environments of storing t, T, and pH, utilizing UV-Visible spectroscopy as the principal investigative method. Time-based stability was assessed by observing the SPR signal at steady intervals—precisely on 1, 5, 9, 13, 15, and 120 days —whereas trials were stowed in airtight glass bottles under dark environments. The retention or move in SPR features over time offered understanding into the nanoparticles long-term colloidal

http://www.doi.org/10.62341/smza1125

stability. Thermal stability was evaluated by exposing the AgNPs suspensions to precise heating system at four dissimilar temperatures: 25°C, 50°C, 80°C, and 100°C. Each trial was subjected to heat for 10 minutes, afterwards, UV-Vis absorption spectra were documented to identify any variations in optical characters, revealing of thermal-induced aggregation or structural alteration. Additionally, the effect of pH on nanoparticle stability was scanned by regulating the pH of the AgNP solutions to values—1, 2, 4, 7, 8, 9, and 13— range using 0.1 N hydrochloric acid and 0.1 N sodium hydroxide. The resultant UV-Vis spectra were collected for each pH state to estimate the stability and aggregation propensity of the nanoparticles under both acidic and alkaline backgrounds. This multifactorial approach enabled a comprehensive understanding of the physicochemical strength of AgNPs under dissimilar environmental conditions.

Assessment of Antibacterial Capability

The in vitro antimicrobial capability of the manufactured silver nanoparticles was statistically estimated versus a Gram-negative bacterial strain of *Escherichia coli* utilizing the consistent disc diffusion technique. The microbial strain was acquired from the zoology department at Sebha University. For culturing the bacteria, Mueller-Hinton (M.H) agar at a concentration of 38 g/L and nutrient broth (N.B) at 25 g/L were utilized to provide optimal growth conditions and reliable test results. In this study, the antimicrobial capability of synthesized silver nanoparticles versus *Escherichia coli* was assessed utilizing the dilution means. A sequences of standard antibiotics—Amoxicillin, Kanamycin, Tetracycline, Nalidixic acid, Polymyxin B, and Chloramphenicol—were utilizing as reference controls to compare the inhibition effectiveness of AgNPs. To achieve the antibacterial assay, sterile paper discs were soaked with 100 µL of AgNP suspensions, each matching to diverse initial concentrations of silver nitrate employed in their production. The ready discs were carefully positioned on agar dishes infected with *E. coli* and then cultured at 37°C for a age ranging from 24 to 48 hours. Subsequent the growth, the antibacterial effect was evaluated by assessing the diameter of the distinct regions of inhibition shaped nearby each disc, which specifies the degree of bacterial growth conquest. This procedure delivered quantifiable

http://www.doi.org/10.62341/smza1125

insights into the ability of AgNPs as antimicrobial agents and assisted valuation across various concentrations.

Results and Discussion

Synthesis and Characterization

The fruitful production of silver nanoparticles was primarily inveterate over a visible color alteration in the reaction combination—from light yellow to variable shadows of brown—matching the nucleation and progress of nanoparticles formation (Figure 2) (Aisha Al-Abbasi & Sida, 2024; Umadevi, Shalini, & Francis, 2012). This color transition is a firm optical sign of AgNP construction, attributed to surface plasmon resonance occurrences. Supplementary approval was acquired through UV-Visible spectroscopy, which showing separate and distinct SPR absorption bands centred around 400 nm (Tiara Egga, Windri, & Cuk, 2021; Titus, James Jebaseelan Samuel, & Roopan, 2019). These spectral features are representative of colloidal silver nanoparticles and serve as evidence of their successful formation and dispersion in solution. Moreover, the strength of the absorption signals increased consistently with the concentration of silver nitrate, demonstrating that higher precursor concentrations directed to the establishment of a superior number of nanoparticles with boosted optical density (Aziz, Abdullah, Saber, Rasheed, & Ahmed, 2017).

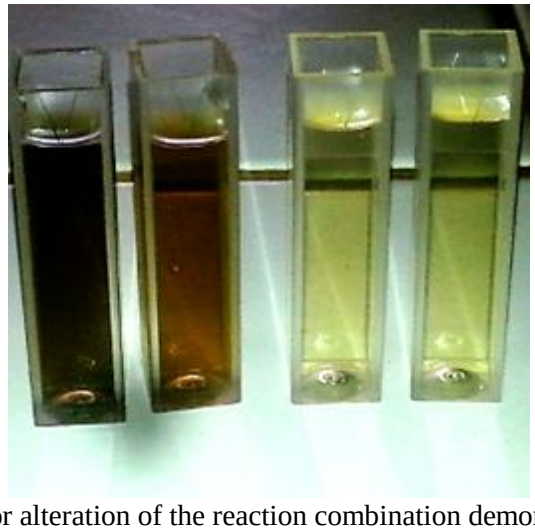

Fig. 2: Color alteration of the reaction combination demonstrating the establishment of nano silver

http://www.doi.org/10.62341/smza1125

Effect of Primary Silver Nitrate Concentration

SPR peaks moved and strengthened with increasing silver nitrate concentration (Figure 3). Weak absorptions (0.07 and 0.38 $L \cdot mol^{-1} \cdot cm^{-1}$) were detected at 411 and 401 nm for 0.1 and 0.2 mM, respectively. A sharp peak (3.57 $L \cdot mol^{-1} \cdot cm^{-1}$) observed at 393 nm for 1.0 mM, indicating a higher yield of nanoparticles (Sobczak-Kupiec, Malina, Wzorek, & Zimowska, 2011).

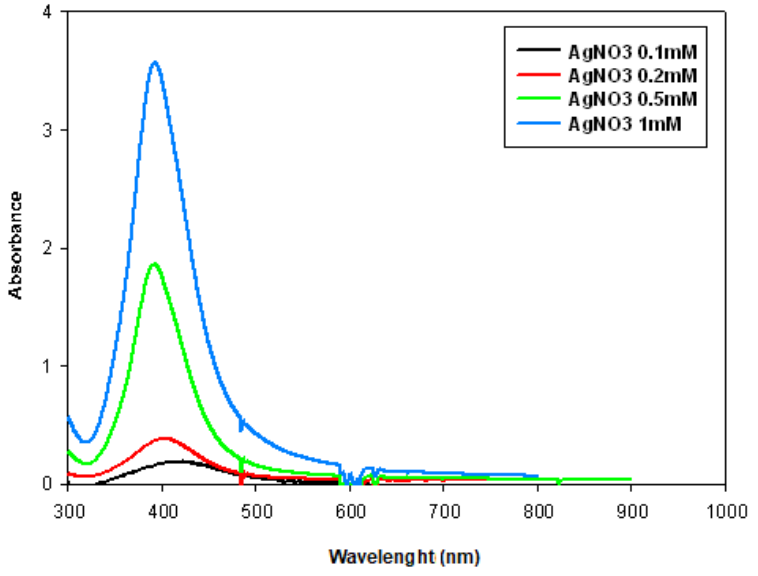

Fig. 3: UV/vis spectra of the nano silver particles manufactured by $AgNO_3$ reduction

Effect of Time

Fig. 4 shows the evolution of surface plasmon resonance (SPR) bands, which are a direct indicator of nanoparticle size, distribution, and aggregation state. The UV-visible absorption spectra of AgNPs are stored over a range of time intervals, from one day to three months. Panel (a) at 0.1 mM: This subplot tracks the UV-Vis absorption of AgNPs over a short duration (1, 5, and 9 days). A consistent increase in absorption intensity is noticed over time, with the SPR peak becoming more noticeable and marginally red-shifted. This recommends enhanced dispersion or particle growth during the early storing phase. The inset plot approves the rise in absorption intensity, demonstrating a possible increase in particle number or uniformity in size distribution up to day 9. Panel (b) 0.2 mM: Here, the data spans a longer duration (1 day to 3 months) (Baiee, Liu, &

http://www.doi.org/10.62341/smza1125

Li, 2019). The SPR peak is still apparent but after the third month in particular, the peak intensity gradually decreases in its intensity, and the λ_{max} shifts red.

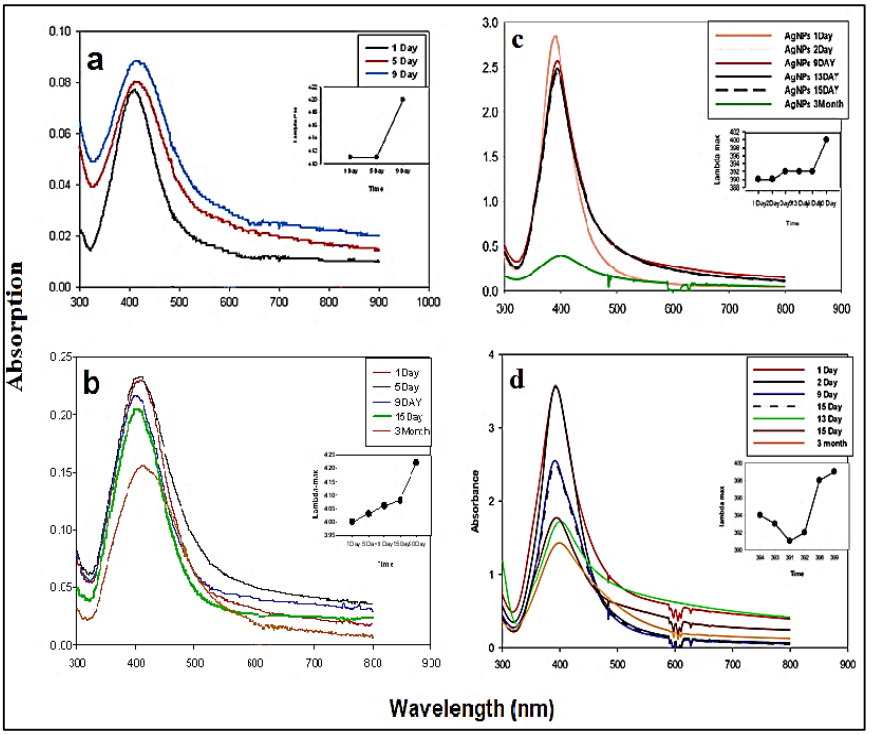

Fig. 4: The permanence of AgNPs throughout time at: a) 0.1 mM, b) 0.2 m, c) 0.5 mM, d) 1 mM of $AgNO_3$

This specifies progressive agglomeration or partial degradation of nanoparticle stability. The inset approves a slow rise in λ_{max} values over time, signaling a shift toward larger or more aggregated particles (Baiee et al., 2019). Panel (c) 0.5 mM: This plot shows a high-concentration AgNP sample over a similar time range. Unlike earlier graphs, the absorption peak declines sharply at day 9, signifying potential instability or aggregation at this concentration. However, the peak reappears and intensifies again at day 30 and 3 months. This could be attributed to sedimentation-resuspension effects or dynamic restructuring in the colloidal medium (El Badawy, Scheckel, Suidan, & Tolaymat, 2012). The inset trend of λ_{max} values supports the idea of nonlinear particle evolution, with potential oscillation between aggregation and partial redispersion.

http://www.doi.org/10.62341/smza1125

Panel (d) 1 mM: This plot represents the highest recorded absorbance among all panels, likely corresponding to the highest $AgNO_3$ concentration. The initial days (1–9) show increasing intensity and a stable SPR peak, reflecting good short-term stability. By day 30 and 90, however, there's a reduction in intensity and minor red-shifting, suggesting some degree of particle interaction or clustering. The inset trend of λ_{max} again approves the red shift, consistent with reasonable aggregation.

Influence of Temperature

As the temperature rises from 25°C to 50°C to 80°C to 100°C, the UV-Vis absorption spectra displayed in Figure 5(a–d) illustrate how silver nanoparticles, which were synthesised at different initial concentrations of $AgNO_3$, react to thermal stress.

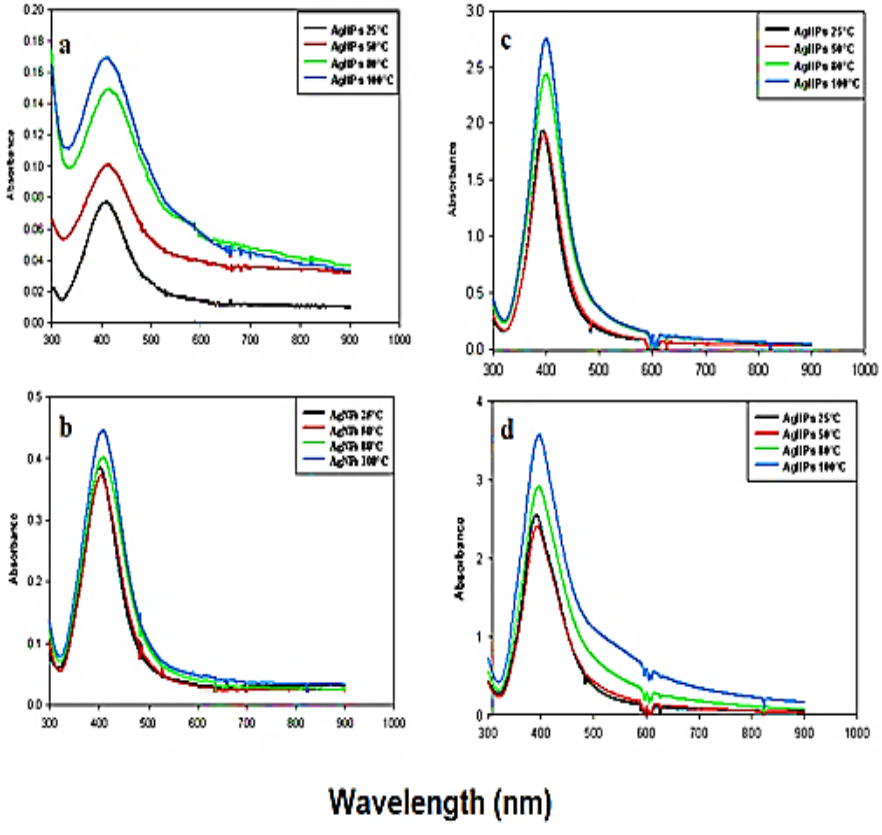

Fig. 5: The correlation involving temperature at: a) 0.1 mM, b) 0.2 m, c) 0.5 mM, d) 1 mM of $AgNO_3$

http://www.doi.org/10.62341/smza1125

By monitoring the strength and location of the surface plasmon resonance (SPR) peak, which is normally located between 400 and 420 nm, these spectra shed light on the optical behaviour, particle stability, and possible aggregation of AgNPs under various heat circumstances. 0.1 mM in As the temperature rises from 25, 50, 80, 100 °C, the UV-Vis absorption spectra displayed in Figure 5(a–d) show how silver nanoparticles, which were produced at various starting amounts of $AgNO_3$, react to thermal stress. By monitoring the strength and location of the SPR peak, which typically faeen 400 and 420 nm, these spectra shed light on the optical behaviour, particle stability, and possible aggregation of AgNPs under various heat settings. 0.1 mM in Panel (a): Data for the lowest $AgNO_3$ concentration (probably 0.1 mM) are shown in this plot (A. A. Al-abbasi & Kassim, 2011; A. A. Al-abbasi, Mohamed Tahir, & Kassim, 2012; El Badawy et al., 2012). Panel (b) 0.2 mM: For a slightly higher $AgNO_3$ concentration, the trend remains similar: absorbance increases with temperature, and the SPR peak remains sharp and prominent. However, the shifts in peak position are more subtle, indicating moderate structural rearrangement without severe aggregation (A. Al-abbasi, Belkher, Ahmida, & Zidan, 2023; Hashemi Zadeh, Rashidi-Huyeh, & Palpant, 2017). The nanoparticles seem to maintain their colloidal stability even at 100°C, supported by stable, high-intensity absorbance profiles. Panel (c) 0.5 mM: At a still higher concentration of $AgNO_3$ (e.g., 0.5 mM), the spectral response shows a significant increase in absorbance with temperature. The SPR peak becomes more intense and slightly narrower with rising temperatures, especially between 50°C and 100°C. The persistence of a defined peak in this concentration range suggests that thermal energy may enhance nanoparticle dispersion or prevent agglomeration by improving the surfactant (SDS) coverage on particle surfaces (González, Noguez, Beránek, & Barnard, 2014).

Panel (d) 1 mM: At the highest $AgNO_3$ concentration (likely 1.0 mM), the SPR peak is extremely intense and shifts slightly toward longer wavelengths (red-shift) as the temperature rises. While this could indicate some degree of aggregation or particle growth, the overall peak shape remains narrow and distinct, which confirms that the nanoparticles retain colloidal stability even under high thermal conditions. The increased absorbance at higher temperatures may

http://www.doi.org/10.62341/smza1125

also reflect enhanced particle concentration or a more uniform size distribution.

pH Influence

Figure 6 demonstrates the influence of pH values ranging from 1 to 13 on the SPR and absorbance behavior Ag nano, which are sensitive displays of their colloidal stability, and amount of aggregation.

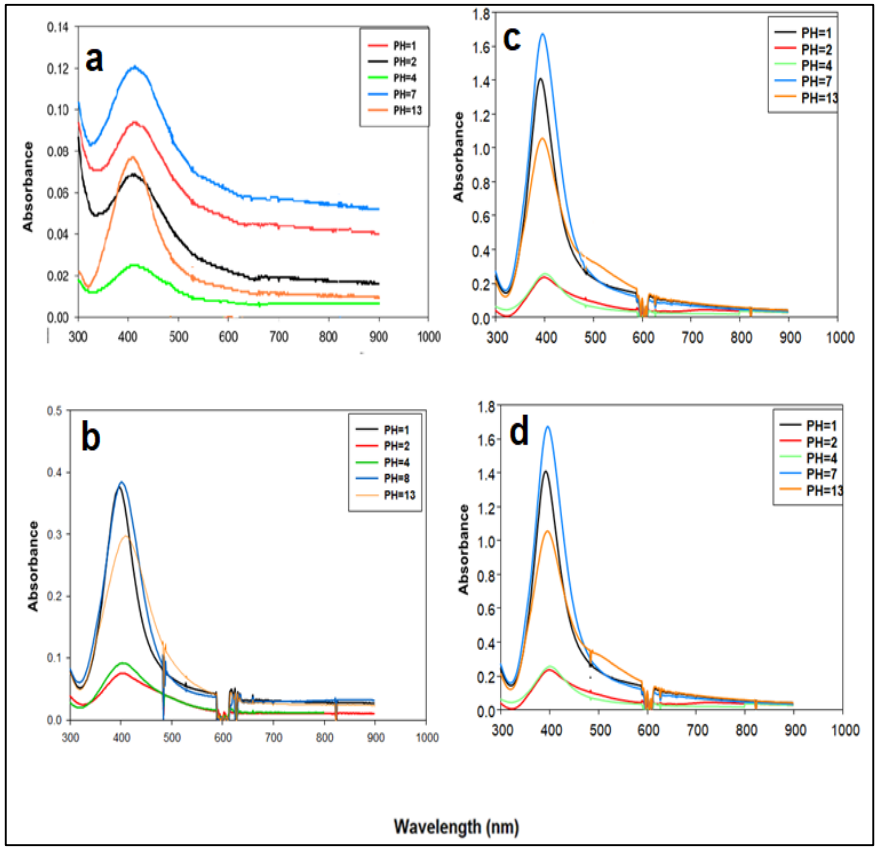

Fig. 6: The impact of pH on AgNP stability at: a) 0.1 mM, b) 0.2 m, c) 0.5 mM, d) 1 mM of $AgNO_3$

The SPR signal typically appear between 400–420 nm, and their shape, position, and intensity change under changing pH environments. Panel (a) 0.1 mM: This panel shows the effect of pH values 1, 2, 4, 7, and 13 at low AgNP concentration. The highest SPR peak intensity is observed at pH 7, indicating optimal

http://www.doi.org/10.62341/smza1125

nanoparticle stability under neutral conditions. At pH 4, the absorbance drops significantly, suggesting aggregation or dissolution of particles. At pH 13, despite an increase in intensity, the peak becomes broader, possibly indicating particle growth or irregular distribution.

The acidic environment (pH 1–2) shows moderate stability but less than that of neutral pH. Panel (b) 0.2 mM: Here, the SPR peaks at pH 8 and 13 are more pronounced than in acidic environments. The sharpness and symmetry of the SPR peak at pH 8 indicate a slightly better dispersion than at pH 13. Acidic pH (especially pH 4) shows poor absorbance, again indicating instability. This suggests that mildly alkaline conditions may also support AgNP stability, though not as well as neutral pH (Suhud et al., 2015; Velgosová et al., 2018).

Panel (c) 0.5 mM: This subplot, likely corresponding to a higher AgNP concentration, confirms the previous trend. The narrowest and most intense SPR peak appears at pH 7, affirming that neutral pH favors well-dispersed, uniformly sized nanoparticles. Both extremely acidic (pH 1–2) and alkaline (pH 13) conditions lead to broadened or diminished peaks, suggesting reduced stability or nanoparticle agglomeration. Panel (d) 1 mM: At high nanoparticle concentration, the trend remains consistent: maximum absorbance and optimal SPR shape occur at pH 7, followed closely by pH 13, which shows some red-shifting and broadening. pH 4 again exhibits the lowest absorbance, indicating precipitation, aggregation, or oxidation of nanoparticles.

Antibacterial Activity

The development of inhibiting areas in dilution technique evaluation (Figure 7) clearly showed the antimicrobial ability of silver nanoparticles in combating the Gram-negative bacterium Escherichia coli. As the concentration of AgNPs rose, along with the diameter of these clear areas, indicating a dose-dependent antimicrobial response. In contrast, control tests using sodium borohydride ($NaBH_4$) alone showed no inhibition effect (Figure 8), confirming that the observed antimicrobial capability was solely attributable to the presence of AgNPs (A. Al-abbasi, and Shana, I. , 2021; Vu et al., 2018).

http://www.doi.org/10.62341/smza1125

The antimicrobial action of AgNPs is attributed to their ability to interact electrostatically with bacterial cell membranes. The negatively charged outer surface of *E. coli* cells attracts the positively charged silver nanoparticles, facilitating their adhesion and penetration. Cell death results from this interaction because it seriously compromises membrane integrity, denaturates membrane-bound proteins, and interferes with intracellular functions like DNA replication and enzyme activity. The structural features of Gram-negative bacteria, including their thin peptidoglycan layer and external lipopolysaccharide-rich membrane, make them particularly vulnerable to nanoparticle-mediated damage (Mikhailova, 2025; Vu et al., 2018).

TABLE 1: Antibiotic sensitivity test for *E. coli*

Antibiotic	AML	K	TC	NA	PB	C
Functional Group	**Beta-lactamase**	**Aminoglycoside**	**Tetracycline**	**Quinolones**	**Polypeptide**	**Cephalosporin**
Conc. (µg/ml)	25	30	30	30	300	30
Resistance	R	S	R	R	S	S
Inhibition Zone (mm)	0	20	0	0	10	25

R = Resistance , S = sensitive

Conclusion

Silver nano particles was productively formed using a chemical process involving borohydride sodium salt and SDS. UV-Visible spectral established the production of well-dispersed nano silver, with good surface plasmon resonance signals revealing of their optical stability. The nanoparticles demonstrated excellent stability over time, across a wide temperature range (25–100°C), and under neutral to mildly alkaline pH conditions (pH 7–8). In addition, AgNPs exhibited potent antibacterial capability versus *Escherichia coli*, with a clear dose-dependent inhibition response. Even at low concentrations, the MIC% exceeded 90%, confirming the strong

http://www.doi.org/10.62341/smza1125

antimicrobial potential of AgNPs. Mechanistically, the nano silver particles interrupt bacterial membranes and delay vital cellular procedures, leading to bacterial cell death. Overall, the study establishes the physicochemical robustness and biofunctional utility of silver nanoparticles, validating their application in antimicrobial therapies, biosensors, and environmental disinfectants.

Acknowledgement
Special thanks are due to the Department of Chemistry and the Department of Zoology for their valuable collaboration and guidance throughout the project.

Conflict of Interest
The authors state that they have no interest conflicts.

References
Abbas, R., Luo, J., Qi, X., Naz, A., Khan, I. A., Liu, H., . . . Wei, J. (2024). Silver Nanoparticles: Synthesis, Structure, Properties and Applications. *Nanomaterials, 14*(17), 1425. Retrieved from https://www.mdpi.com/2079-4991/14/17/1425

Ahmed, S., Ahmad, M., Swami, B. L., & Ikram, S. (2016). A review on plants extract mediated synthesis of silver nanoparticles for antimicrobial applications: A green expertise. *Journal of Advanced Research, 7*(1), 17-28. doi:https://doi.org/10.1016/j.jare.2015.02.007

Al-abbasi, A., and Shana, I. . (2021). Corrosion Inhibition of Mild Steel in Acidic Media by Expired Carbimazole Drug. *Journal of Pure & Applied Sciences, 20*(2), 176–180. doi:https://doi.org/10.51984/jopas.v20i2.1646

Al-abbasi, A., Belkher, N., Ahmida, K., & Zidan, M. (2023). Potentiometric Studies on Binary and Ternary Complexes of Ni(II) and Cu(II) Ions with L-Valine and Paracetamol. *Journal of the Turkish Chemical Society Section A: Chemistry, 10*(2), 325-338. doi:10.18596/jotcsa.1140039

Al-Abbasi, A., & Sida, H. (2024). Colorimetric evaluation of the corrosion rate of steel in acidic media in the presence of pentoxifylline drug and KI. *Int. J. Corros. Scale Inhib., 13*(2), 995-1011. doi:10.17675/2305-6894-2024-13-2-19

http://www.doi.org/10.62341/smza1125

Al-abbasi, A. A., & Kassim, M. B. (2011). 1-Benzoyl-3-ethyl-3-phenylthiourea. *Acta Crystallographica Section E, 67*(3), o611. doi:doi:10.1107/S1600536811004326

Al-abbasi, A. A., Mohamed Tahir, M. I., & Kassim, M. B. (2012). N-(Pyrrolidin-1-ylcarbothioyl)benzamide. *Acta Crystallographica Section E, 68*(1), o201. doi:doi:10.1107/S1600536811053694

Ali, M. I., Omar, M. E., & Al-Abbasi, A. A. (2025). Removal of silver nanoparticles from aqueous solution using cellulose extracted from Traganum Nudatum plant activated by zinc chloride. *Next Nanotechnology, 7*, 100190. doi:https://doi.org/10.1016/j.nxnano.2025.100190

Almutaleb, A., & Alabbasi, A. (2023). Synthesis, characterization and computational studies for (2′S*,3R*,3′S*,8a′R*)-2′,3′-bis(ethoxycarbonyl)-2-oxo-2′,3′-dihydro-8a′H-spiro[indoline-3,1′-indolizine]-6′-carboxylic acid and some derivatives. *Journal of Physical Organic Chemistry, 36*(2), e4452. doi:https://doi.org/10.1002/poc.4452

Anees Ahmad, S., Sachi Das, S., Khatoon, A., Tahir Ansari, M., Afzal, M., Saquib Hasnain, M., & Kumar Nayak, A. (2020). Bactericidal activity of silver nanoparticles: A mechanistic review. *Materials Science for Energy Technologies, 3*, 756-769. doi:https://doi.org/10.1016/j.mset.2020.09.002

Aziz, S. B., Abdullah, O. G., Saber, D. R., Rasheed, M. A., & Ahmed, H. M. (2017). Investigation of Metallic Silver Nanoparticles through UV-Vis and Optical Micrograph Techniques. *International Journal of Electrochemical Science, 12*(1), 363-373. doi:https://doi.org/10.20964/2017.01.22

Baiee, R., Liu, Z., & Li, L. (2019). Understanding the stability and durability of laser-generated Ag nanoparticles and effects on their antibacterial activities. *Advances in Natural Sciences: Nanoscience and Nanotechnology, 10*(3), 035001. doi:10.1088/2043-6254/ab2e6e

Bruna, T., Maldonado-Bravo, F., Jara, P., & Caro, N. (2021). Silver Nanoparticles and Their Antibacterial Applications. *Int J Mol Sci, 22*(13). doi:10.3390/ijms22137202

Carlson, C., Hussain, S. M., Schrand, A. M., Braydich-Stolle, L. K., Hess, K. L., Jones, R. L., & Schlager, J. J. (2008). Unique cellular interaction of silver nanoparticles: size-dependent generation of

http://www.doi.org/10.62341/smza1125

reactive oxygen species. *J Phys Chem B, 112*(43), 13608-13619. doi:10.1021/jp712087m

Dhaka, A., Chand Mali, S., Sharma, S., & Trivedi, R. (2023). A review on biological synthesis of silver nanoparticles and their potential applications. *Results in Chemistry, 6*, 101108. doi:https://doi.org/10.1016/j.rechem.2023.101108

Dnkm, A., Al-Abbassi, A., & Erhayem, M. (2024). Synthesis and Characterization of Silver Nanoparticles Using Amberlite LA-2 Functionalized with Benzoyl Thiourea as a Capping Agent. *Chemistry Africa*. doi:10.1007/s42250-024-00902-9

Duman, H., Eker, F., Akdaşçi, E., Witkowska, A. M., Bechelany, M., & Karav, S. (2024). Silver Nanoparticles: A Comprehensive Review of Synthesis Methods and Chemical and Physical Properties. *Nanomaterials, 14*(18), 1527. Retrieved from https://www.mdpi.com/2079-4991/14/18/1527

El Badawy, A. M., Scheckel, K. G., Suidan, M., & Tolaymat, T. (2012). The impact of stabilization mechanism on the aggregation kinetics of silver nanoparticles. *Science of The Total Environment, 429*, 325-331. doi:https://doi.org/10.1016/j.scitotenv.2012.03.041

Emma, L. (2025). Nanotechnology and Its Applications in Science and Engineering.

Fernando, I. (2018). Impact of pH on the stability, dissolution and aggregation kinetics of silver nanoparticles. *Chemosphere, 216*. doi:10.1016/j.chemosphere.2018.10.122

González-Fernández, S., Blanco-Agudín, N., Rodríguez, D., Fernández-Vega, I., Merayo-Lloves, J., & Quirós, L. M. (2025). Silver Nanoparticles: A Versatile Tool Against Infectious and Non-Infectious Diseases. *Antibiotics, 14*(3), 289. Retrieved from https://www.mdpi.com/2079-6382/14/3/289

González, A. L., Noguez, C., Beránek, J., & Barnard, A. S. (2014). Size, Shape, Stability, and Color of Plasmonic Silver Nanoparticles. *The Journal of Physical Chemistry C, 118*(17), 9128-9136. doi:10.1021/jp5018168

Güzel, R., & Erdal, G. (2018). Synthesis of Silver Nanoparticles. In M. Khan (Ed.), *Silver Nanoparticles - Fabrication, Characterization and Applications*. Rijeka: IntechOpen.

Haleem, A., Javaid, M., Singh, R. P., Rab, S., & Suman, R. (2023). Applications of nanotechnology in medical field: a brief review.

http://www.doi.org/10.62341/smza1125

Global Health Journal, 7(2), 70-77. doi:https://doi.org/10.1016/j.glohj.2023.02.008

Haque, M. N. (2017). Formation and stability study of silver nano-particles in aqueous and organic medium. *Korean Journal of Chemical Engineering, 34*. doi:10.1007/s11814-017-0096-z

Hashemi Zadeh, S., Rashidi-Huyeh, M., & Palpant, B. (2017). Enhancement of the thermo-optical response of silver nanoparticles due to surface plasmon resonance. *Journal of Applied Physics, 122*(16). doi:10.1063/1.4997276

Hosseini, M., Moghaddam, L., Barner, L., Cometta, S., Hutmacher, D. W., & Medeiros Savi, F. (2025). The multifaceted role of tannic acid: From its extraction and structure to antibacterial properties and applications. *Progress in Polymer Science, 160*, 101908. doi:https://doi.org/10.1016/j.progpolymsci.2024.101908

Jayaram, U., & Gurusamy, A. (2018). *Biosynthesis and Characterization of Silver Nanoparticles Using Leaf Extract Abutilon indicum*.

Mavani, K., & Shah, M. (2013). *Synthesis of Silver Nanoparticles by using Sodium Borohydride as a Reducing Agent*.

Mikhailova, E. O. (2025). Green Silver Nanoparticles: An Antibacterial Mechanism. *Antibiotics, 14*(1), 5. Retrieved from https://www.mdpi.com/2079-6382/14/1/5

More, P. R., Pandit, S., Filippis, A., Franci, G., Mijakovic, I., & Galdiero, M. (2023). Silver Nanoparticles: Bactericidal and Mechanistic Approach against Drug Resistant Pathogens. *Microorganisms, 11*(2). doi:10.3390/microorganisms11020369

Nasiriboroumand, M., Montazer, M., & Barani, H. (2018). Preparation and characterization of biocompatible silver nanoparticles using pomegranate peel extract. *Journal of Photochemistry and Photobiology B: Biology, 179*, 98-104. doi:https://doi.org/10.1016/j.jphotobiol.2018.01.006

Nyabadza, A., McCarthy, É., Makhesana, M., Heidarinassab, S., Plouze, A., Vazquez, M., & Brabazon, D. (2023). A review of physical, chemical and biological synthesis methods of bimetallic nanoparticles and applications in sensing, water treatment, biomedicine, catalysis and hydrogen storage. *Advances in Colloid and Interface Science, 321*, 103010. doi:https://doi.org/10.1016/j.cis.2023.103010

http://www.doi.org/10.62341/smza1125

Oleksandra, B., Semeniv, V., Sikorska, K., Tetyana, K., Ludmyla, K., & Olena, T. (2021). SYNTHESIS AND PROPERTIES OF NEW NANOSYSTEMS OF ARGENTUM. *Ukrainian Chemistry Journal, 87*(2). doi:10.33609/2708-129X.87.02.2021.95-106

Rodrigues, A. S., Batista, J. G. S., Rodrigues, M. Á. V., Thipe, V. C., Minarini, L. A. R., Lopes, P. S., & Lugão, A. B. (2024). Advances in silver nanoparticles: a comprehensive review on their potential as antimicrobial agents and their mechanisms of action elucidated by proteomics. *Frontiers in Microbiology, Volume 15 - 2024*. doi:10.3389/fmicb.2024.1440065

S. Khalifa, AL-abbassi, A., & Suliman, M. (2019). Adsorption and Corrosion Inhibition of Mild Steel in Acidic Media by Expired Pharmaceutical Drug. *Journal of Pure & Applied Sciences, 17*(4). doi:10.51984/jopas.v17i4.414

Salim, S. M., Izriq, R., Almaky, M. M., & Al-Abbassi, A. A. (2022). Synthesis and characterization of ZnO nanoparticles for the production of biodiesel by transesterification: Kinetic and thermodynamic studies. *Fuel, 321*, 124135. doi:https://doi.org/10.1016/j.fuel.2022.124135

Sati, A., Ranade, T. N., Mali, S. N., Ahmad Yasin, H. K., & Pratap, A. (2025). Silver Nanoparticles (AgNPs): Comprehensive Insights into Bio/Synthesis, Key Influencing Factors, Multifaceted Applications, and Toxicity─A 2024 Update. *ACS Omega, 10*(8), 7549-7582. doi:10.1021/acsomega.4c11045

Shrestha, S., Wang, B., & Dutta, P. (2020). Nanoparticle processing: Understanding and controlling aggregation. *Advances in Colloid and Interface Science, 279*, 102162. doi:10.1016/j.cis.2020.102162

Sobczak-Kupiec, A., Malina, D., Wzorek, Z., & Zimowska, M. (2011). Influence of silver nitrate concentration on the properties of silver nanoparticles. *Micro & Nano Letters, 6*(8), 656-660. doi:doi:10.1049/mnl.2011.0152

Suhud, K., Heng, L. Y., Rezayi, M., Al-abbasi, A. A., Hasbullah, S. A., Ahmad, M., & Kassim, M. B. (2015). Conductometric Studies of the Thermodynamics for Complexation of 1,1-Diethyl-3-(4-methoxybenzoyl)thiourea and Cobalt(II) Cation in Aqueous Binary Mixtures of Polar Organic Solvents. *Journal of*

http://www.doi.org/10.62341/smza1125

Solution Chemistry, 44(2), 181-192. doi:10.1007/s10953-015-0308-2

Tiara Egga, A., Windri, H., & Cuk, I. (2021, 2021/06/23). *The UV-VIS Spectrum Analysis From Silver Nanoparticles Synthesized Using Diospyros maritima Blume. Leaves Extract.* Paper presented at the Proceedings of the 3rd KOBI Congress, International and National Conferences (KOBICINC 2020).

Titus, D., James Jebaseelan Samuel, E., & Roopan, S. M. (2019). Chapter 12 - Nanoparticle characterization techniques. In A. K. Shukla & S. Iravani (Eds.), *Green Synthesis, Characterization and Applications of Nanoparticles* (pp. 303-319): Elsevier.

Umadevi, M., Shalini, S., & Francis, B. (2012). Synthesis of silver nanoparticle using D. carota extract. *Advances in Natural Sciences: Nanoscience and Nanotechnology, 3*. doi:10.1088/2043-6262/3/2/025008

Velgosova, O., Čižmárová, E., Málek, J., & Kavuličova, J. (2017). Effect of storage conditions on long-term stability of Ag nanoparticles formed via green synthesis. *International Journal of Minerals, Metallurgy, and Materials, 24*(10), 1177-1182. doi:10.1007/s12613-017-1508-0

Velgosová, O., Mražíková, A., Kavuličová, J., Matvija, M., Čižmárová, E., & Willner, J. (2018). Characteristics of Silver Nanoparticles in Different pH Values. *Archives of Metallurgy and Materials, vol. 63*(No 2). doi:10.24425/122433

Vu, X. H., Duong, T. T. T., Pham, T. T. H., Trinh, D. K., Nguyen, X. H., & Dang, V.-S. (2018). Synthesis and study of silver nanoparticles for antibacterial activity against Escherichia coli and Staphylococcus aureus. *Advances in Natural Sciences: Nanoscience and Nanotechnology, 9*(2), 025019. doi:10.1088/2043-6254/aac58f

Wei, L., Lu, J., Xu, H., Patel, A., Chen, Z. S., & Chen, G. (2015). Silver nanoparticles: synthesis, properties, and therapeutic applications. *Drug Discov Today, 20*(5), 595-601. doi:10.1016/j.drudis.2014.11.014

Zhang, X. F., Liu, Z. G., Shen, W., & Gurunathan, S. (2016). Silver Nanoparticles: Synthesis, Characterization, Properties, Applications, and Therapeutic Approaches. *Int J Mol Sci, 17*(9). doi:10.3390/ijms17091534